

Measurement Notes

Note 49

December 1996

**Time Domain Measurement of the Dielectric Properties of Water  
in a Coaxial Test Fixture**

Everett G. Farr  
Farr Research, Inc.

Charles A. Frost  
Pulse Power Physics, Inc.

**Abstract**

We have established a procedure and an apparatus for determining the complex dielectric constant of lossy dielectric materials. The procedure involves impulse transmission through two different lengths of material embedded in a coaxial test fixture. Sample data is taken for distilled water, which has a well-established frequency dependence with a Debye model. The measured data are in good agreement with theory. Measurements on other materials will appear in a later paper.

## I. Introduction

In this note, we develop a methodology and test apparatus for measurements of complex dielectric constants of materials. Measurements are made in a coaxial test fixture, using a time domain technique. Data are taken for distilled water, and are processed to extract the complex dielectric constant. In a later note, we will provide data on other materials.

The measurement of material characteristics in coaxial test fixtures has been of interest for some time. The classic method, proposed by Nicolson and Ross [1], requires measurements of both the reflected and transmitted signal. However, this method requires normalization of both reflected and transmitted signals to a reference plane, and this can introduce noise into the measurement. An improved method, suggested by Courtney et al [2], avoids the need to normalize to a reference plane. However, this method uses D-dot probes to sample the signal in a nonperturbing fashion. D-dot probes provide a significantly lower signal than what would be measured in a direct measurement. Low signal levels can introduce noise into the measurement, especially for materials with high loss.

For the above reasons, we implemented a somewhat different approach, in which we make two transmission measurements through two sample lengths. Since we measure the transmitted signal directly, we have a larger signal than what would be provided by a nonperturbing D-dot probe.

Note, however, that our technique provides only the dielectric constant ( $\epsilon_r$ ), and not the permeability ( $\mu_r$ ). This is in contrast to the other two methods, which measure both quantities. For cases in which the sample is known to be nonmagnetic ( $\mu_r = 1$ ), we expect this will provide a cleaner measurement of dielectric constant, since there will be fewer variables to extract in the data processing.

We begin with the theory used to extract the complex dielectric constant. This is followed by a description of the experimental apparatus, and we conclude with sample data for distilled water. We chose distilled water as a calibration standard because it is well characterized by a simple analytic model. Let us begin now with the theory.

## II. Theory

### A. Calculation of Dielectric Constant

With our measurement technique, we make two separate transmission measurements on an air-filled coaxial transmission-line test fixture. For the first measurement, the fixture contains a material sample of length  $\ell_1$ , and of unknown relative dielectric constant  $\epsilon_r$ . For the second measurement, the sample length is increased to  $\ell_2$ . In both measurements, an identical impulse or step function is launched on one side, and the output is recorded on the other side. The

*relative* transmission measurement, which is the transmitted signal through the long sample normalized to the transmitted signal through the short sample, is

$$\begin{aligned} T_r(\omega) &= e^{-jk_o(\ell_2-\ell_1)(\sqrt{\epsilon_r}-1)} \\ k_o &= \omega / c \end{aligned} \quad (2.1)$$

where we have assumed an  $e^{j\omega t}$  time dependence, and  $c$  is the velocity of light in free space. This is the relative impulse response for pulse propagation through an *additional* amount of material of length  $\ell_2-\ell_1$ , as compared to a similar length air. Note that the above formulation ignores multiple reflections, which are time-gated out of the measurement. To find  $T_r(\omega)$ , one need only calculate the frequency domain ratio of the two time domain measurements, while keeping track of the start times for the first point of each waveform. Note that the Fresnel losses at the dielectric interfaces are identical for the two measurements, so they cancel each other and we do not need to account for them explicitly.

In order to extract the complex dielectric constant from  $T_r(\omega)$ , it is necessary to take the natural logarithm of the calculated impulse response in (2.1), and solve for  $\epsilon_r$ . One must be careful when taking the natural logarithm of  $T_r(\omega)$ , due to phase wraps in the function.

The correct way to implement the logarithm begins by converting the relative transmission coefficient,  $T_r(\omega)$ , to the time domain to unwrap the phase. This is accomplished by rotating the time domain waveform to the left by a time  $\tau_o$ , so its peak occurs at time = 0. This is converted to the frequency domain, and a term of  $-j\omega\tau_o$  is added to the logarithm, to account for the delay that was removed in order to unwrap the phase. Thus, the relative transmission coefficient,  $T_r(\omega)$ , can be expressed in terms of its unwrapped form,  $T_{ru}(\omega)$ , as

$$\begin{aligned} T_r(\omega) &= T_{ru}(\omega) e^{-j\omega\tau_o} \\ \ln(T_r) &= \ln(T_{ru}) - j\omega\tau_o \end{aligned} \quad (2.2)$$

Solving for  $\epsilon_r$ , in (2.1), we now have

$$\epsilon_r(\omega) = \left[ \frac{j \ln[T_{ru}(\omega)] + \omega \tau_o}{k_o(\ell_2 - \ell_1)} + 1 \right]^2 \quad (2.3)$$

and we have our final solution for the complex dielectric constant as a function of frequency. Note that with the time convention we are using, the imaginary part of  $\epsilon_r$  is normally less than zero.

## B. Attenuation Constant Calculation

Let us now consider how to express the measured dielectric constant in terms of an attenuation per unit length. We begin by expressing the impulse response (propagation factor) of a layer of media with thickness  $\Delta z$  and dielectric constant  $\epsilon_r$  as

$$\begin{aligned} T(\omega) &= e^{-j\sqrt{\epsilon_r(\omega)}k_o\Delta z} = e^{-n''k_o\Delta z} \times e^{-jn'k_o\Delta z} \\ n(\omega) &= \sqrt{\epsilon_r(\omega)} \\ &= n'(\omega) - jn''(\omega), \quad n' \text{ \& } n'' \text{ are real} \end{aligned} \quad (2.4)$$

where  $n(\omega)$  is the complex index of refraction. The attenuation coefficient is the first factor in the above impulse response. To convert to attenuation in decibels, we use the formula

$$\begin{aligned} \alpha|_{dB} &= -20 \log_{10}\left(e^{-n''(\omega)k_o \times \Delta z}\right) \\ &= 20 n''(\omega) k_o \Delta z \log_{10}(e) \\ &= 8.686 n''(\omega) k_o \Delta z \end{aligned} \quad (2.5)$$

Thus, an attenuation for a 1 cm slab is expressed in dB/cm as

$$\begin{aligned} \alpha|_{dB/cm} &= 8.686 k_o n''(\omega) \times 0.01 \text{ cm / m} \\ &= 0.0868 k_o n''(\omega) \end{aligned} \quad (2.6)$$

where  $k_o$  is expressed in radians/m. This is the final result.

## C. The Debye Model for Water

Since we chose water as a calibration standard, we review here the Debye model for the dielectric constant of water. In the frequency domain, this is expressed as [3]

$$\epsilon_r(\omega) = \epsilon_\infty + \frac{\epsilon_s - \epsilon_\infty}{1 + j\omega t_o} \quad (2.7)$$

where  $\epsilon_\infty$  is the relative dielectric constant at high frequencies,  $\epsilon_s$  is the relative dielectric constant at low frequencies, and  $t_o$  is the relaxation time for water. Furthermore, according to [3], the three constants are  $\epsilon_\infty = 1.8$ ,  $\epsilon_s = 81$ , and  $t_o = 9.4$  ps. Note that there is some variation in these parameters with temperature and pressure, so this model can only be considered a good approximation. This is the model to which we will later compare.

### III. Experimental Measurement Technique

Our time domain measurement technique utilizes the propagation of plane wave pulses in a coaxial transmission line containing uniform samples of the lossy dielectric. The incident, reflected, and transmitted pulses are all observed with picosecond resolution using a sampling oscilloscope. Various pulse shapes including step, impulse, and doublet, can be used. The source amplitude, risetime, and pulse width can be controlled by the experimenter to study the effect of pulse parameters on propagation. The apparatus was checked out in both TDR and transmission mode using (once-) distilled water as the known calibration standard. Both step and impulse waveshapes were employed and found to give consistent results.

The 1 meter long coaxial transmission line propagation section was built with a large diameter so that the granularity of sand and soil samples is averaged out over the measurement volume. The effects of voids and microporosity are thus sampled in a realistic manner. A conical wave expansion section is used to launch a plane wave into the large diameter propagation section.

The apparatus can be used in two modes. These are the TDR (time domain reflectometer) mode and the transmission mode. Figure 3.1 shows an example of the measurement setup used for the TDR mode. A fast rising step pulse from the pulse generator passes through a feed-through sampling head to the conical wave expansion section which allows a smooth increase of the coaxial transmission line diameter without exciting non-TEM modes. The plane wave propagates along the air-filled coaxial line propagation section to a planar interface with the lossy dielectric material. A reflection from the interface travels back to the feedthrough sampling head where it is measured. The primary wave propagates through the dielectric to a planar short circuit termination at the end of the line. The reflection from the planar short then passes back through the dielectric to the sampling head. An analysis of the second reflection, which has passed through the dielectric twice, gives an independent measurement of the dielectric properties of the material. Thus, we can determine both reflection and transmission characteristics with the TDR apparatus. The TDR mode is also referred to as a reflection mode measurement.

The second operating mode is the transmission mode, in which the pulse passes through the sample and is measured at the opposite end. Reflected waves are not measured, and we generally use a resistive attenuator on the input side of the coaxial line fixture to absorb the reflected waves before they reach the source. Figure 3.2 shows an example of the measurement setup as used for the transmission mode. In transmission mode an expansion cone is used for both the entrance and exit ends of the transmission line. The pulse is launched into the line, passes through the sample as a plane wave, and is measured after exiting the far side.

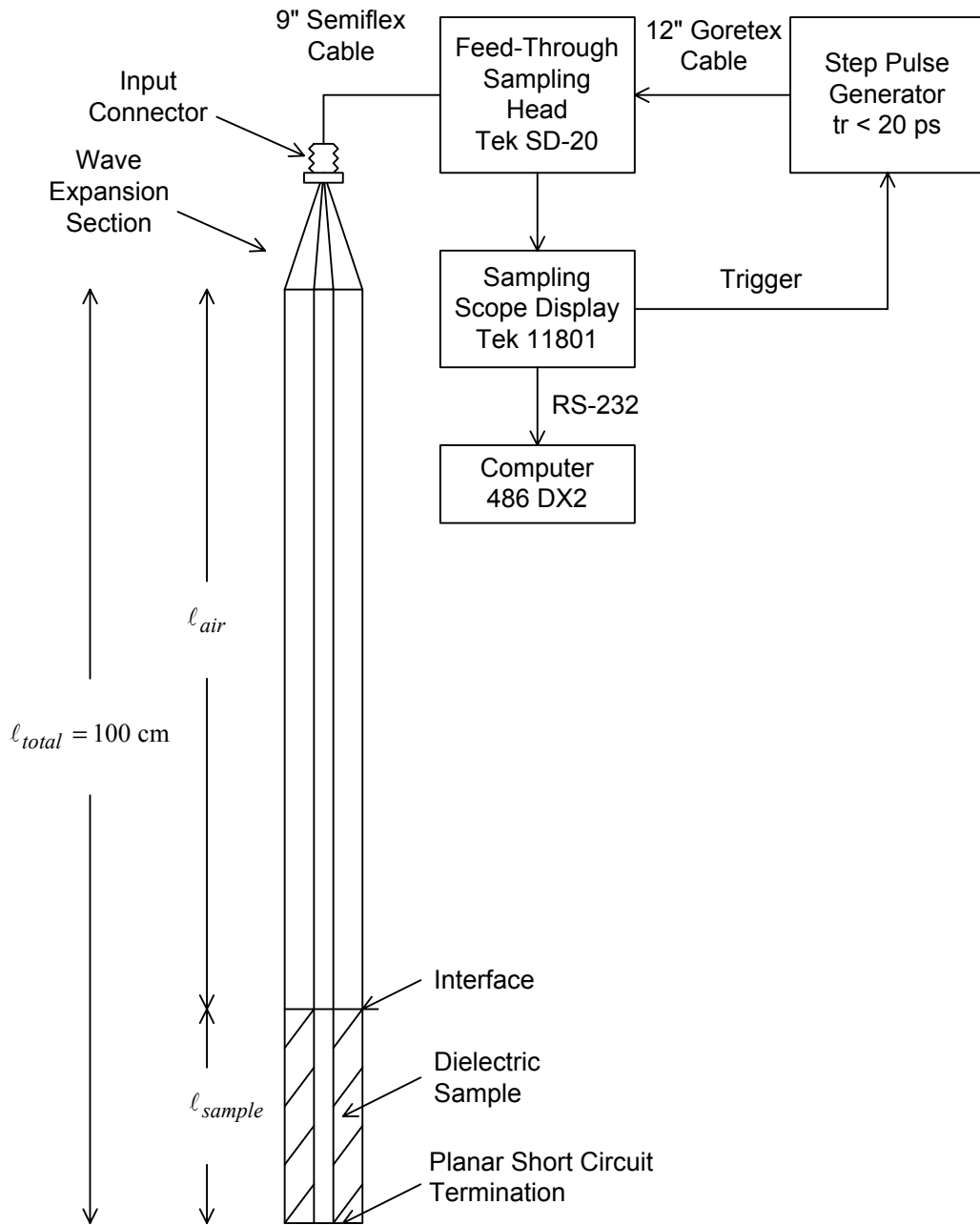


Figure 3.1. Instrumentation setup for measurements in TDR mode.

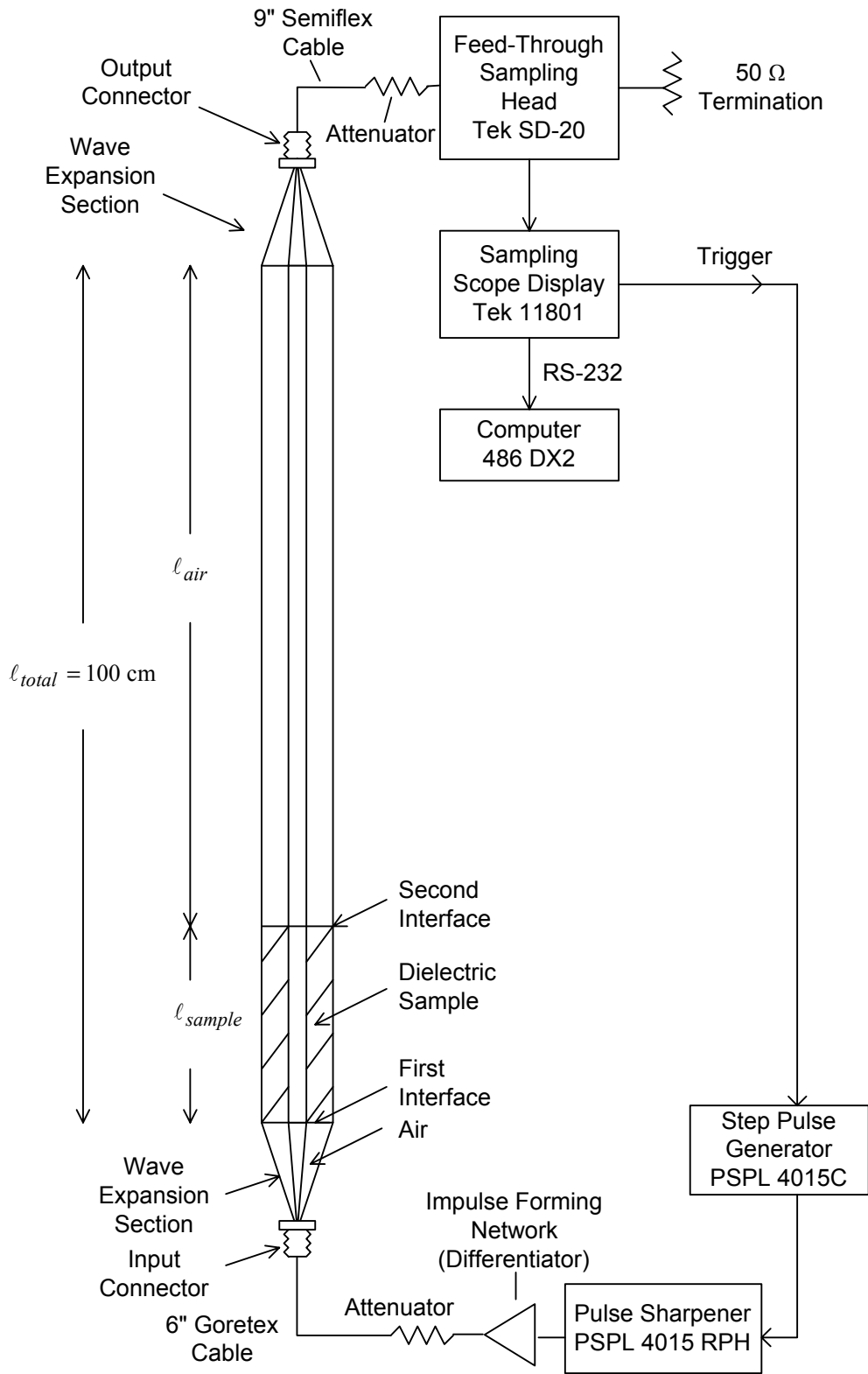


Figure 3.2. Instrumentation setup for measurements in transmission mode with impulse waveshape.

The transmitted pulse is modified by a characteristic time delay, attenuation, and dispersion. The constitutive parameters of the lossy dielectric materials are determined from the way in which the pulse shape is modified by propagation. We use multiple (at least two) measurements with different lengths of material in the transmission line to remove the effects of Fresnel losses at entry and exit interfaces to the dielectric material. We look at the changes in pulse shape which occur for propagation through two different lengths of material. We will describe the apparatus in more detail in the following sections. We will next describe the coaxial test fixture in detail.

### **A. Coaxial Test Fixture**

Figure 3.3 shows the overall physical appearance of the coaxial transmission line apparatus. The transmission line is mounted vertically so that the interface between air and liquid or powder samples is perpendicular to the wave propagation direction. The coaxial line is basically a 1 meter length of high quality air dielectric, 50 ohm coaxial transmission line within which material samples can be placed for measurement. End caps with connectors allow the pulses to enter and leave the line. The end caps are held together by three sets of coil springs which provide the force necessary to maintain good electrical contact between the conductors. The line has very thin dielectric barriers spaced 100.0 cm apart so that the liquid, powder, or granular material samples will be constrained within the line. The barriers are made of 20 mil thick polycarbonate, which gives minimal wave perturbation yet is strong enough to contain heavy samples. The total length of the apparatus is actually longer than 100 cm due to the input and output conical expansion transition sections.

The line is fabricated from precision (drawn over mandrel) reactor grade brass tubing. This tubing provides a 1.59 cm (0.625 in) inner conductor outer diameter and a 3.632 cm (1.430 in) outer conductor inner diameter with a tolerance of less than  $2.54 \times 10^{-3}$ cm (0.001 in) and high degree of concentricity.

Perhaps the most critical element for measurement accuracy is the conical expansion section. Figure 3.4 shows a detailed rendering of this key element. The input connector is a modified type OSM flange jack with extended Teflon dielectric which forms a 50 ohm coax line when surrounded with a tight fitting conducting tube. We modified the jack by threading the end pin with a very fine (1.20 UNM) thread which is screwed directly into the inner cone extension.

The rate of cone expansion is sized (with a tolerance of 1 mil) for a constant 50 ohm impedance over the entire length. The expansion length is calculated to keep the waveform dispersion below 20 picoseconds and thus launch a plane wave into the 100 cm propagation region within which the samples are placed. Any length of sample from 0 to 100 cm can be contained within the propagation region. The design uses silver loaded conducting elastimer O-ring seals to maintain a continuous (constant radius) low inductance current path for the inner and outer conductors. The O-rings are shown as items 11 and 12 in Figure 3.4. The transmission mode apparatus has two identical expansion sections, one for the wave entering and one for the wave exiting the propagation section.

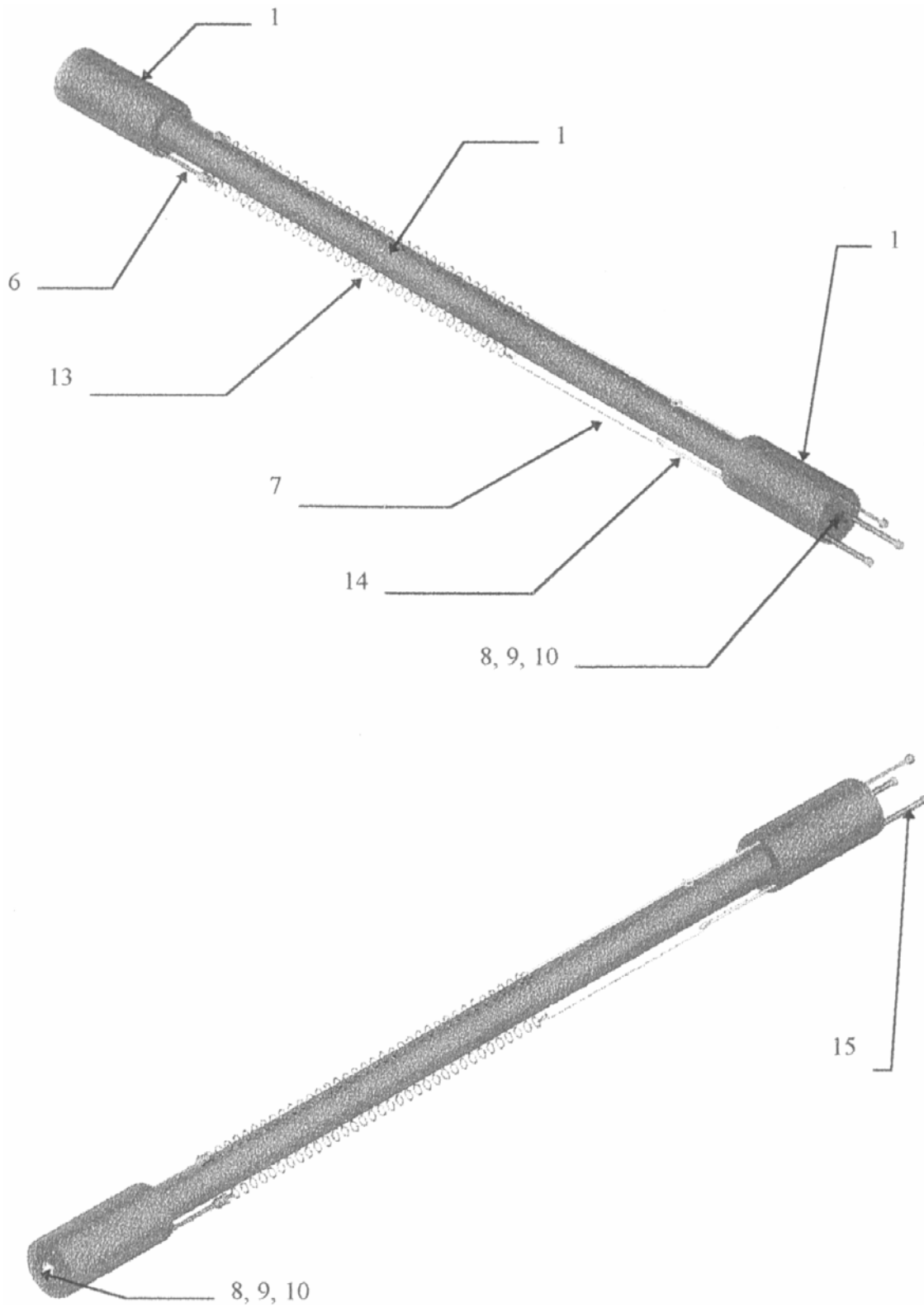


Figure 3.3. Coaxial transmission line apparatus.

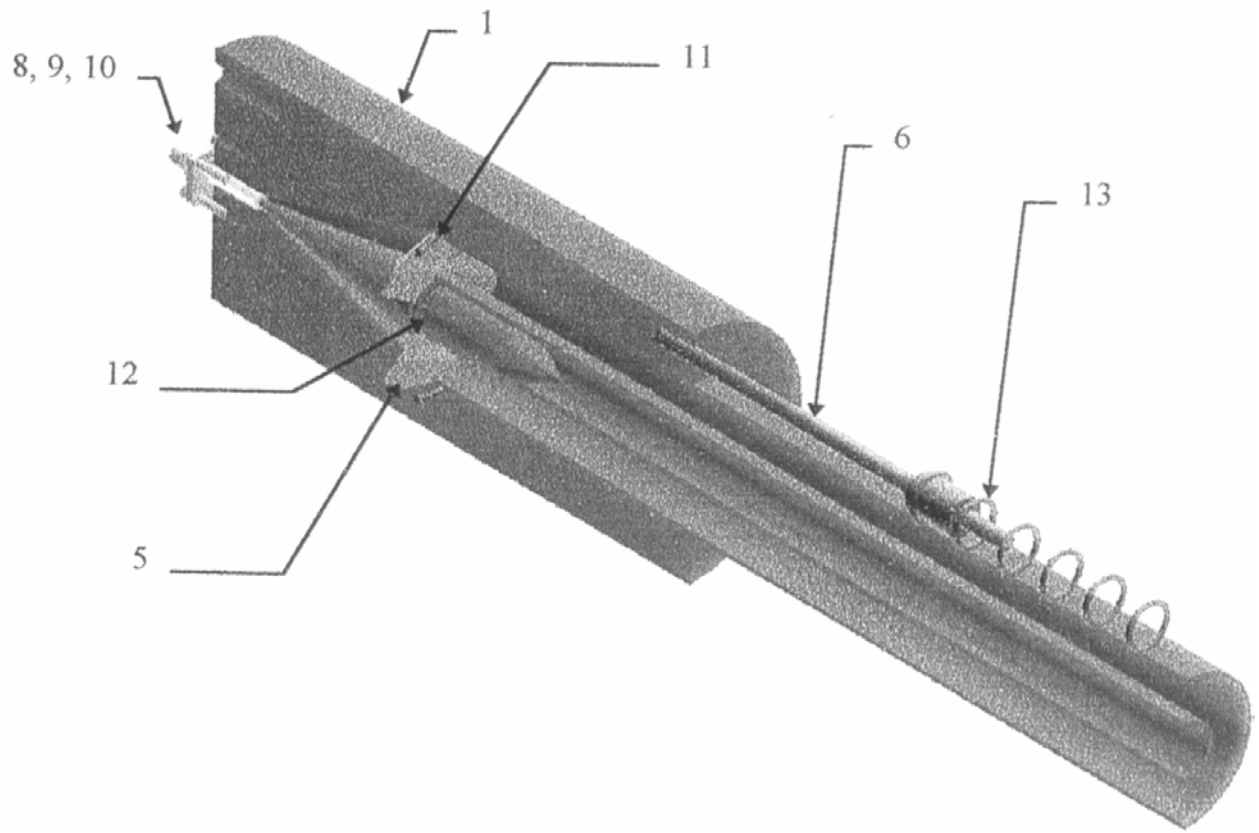


Figure 3.4. Conical expansion section.

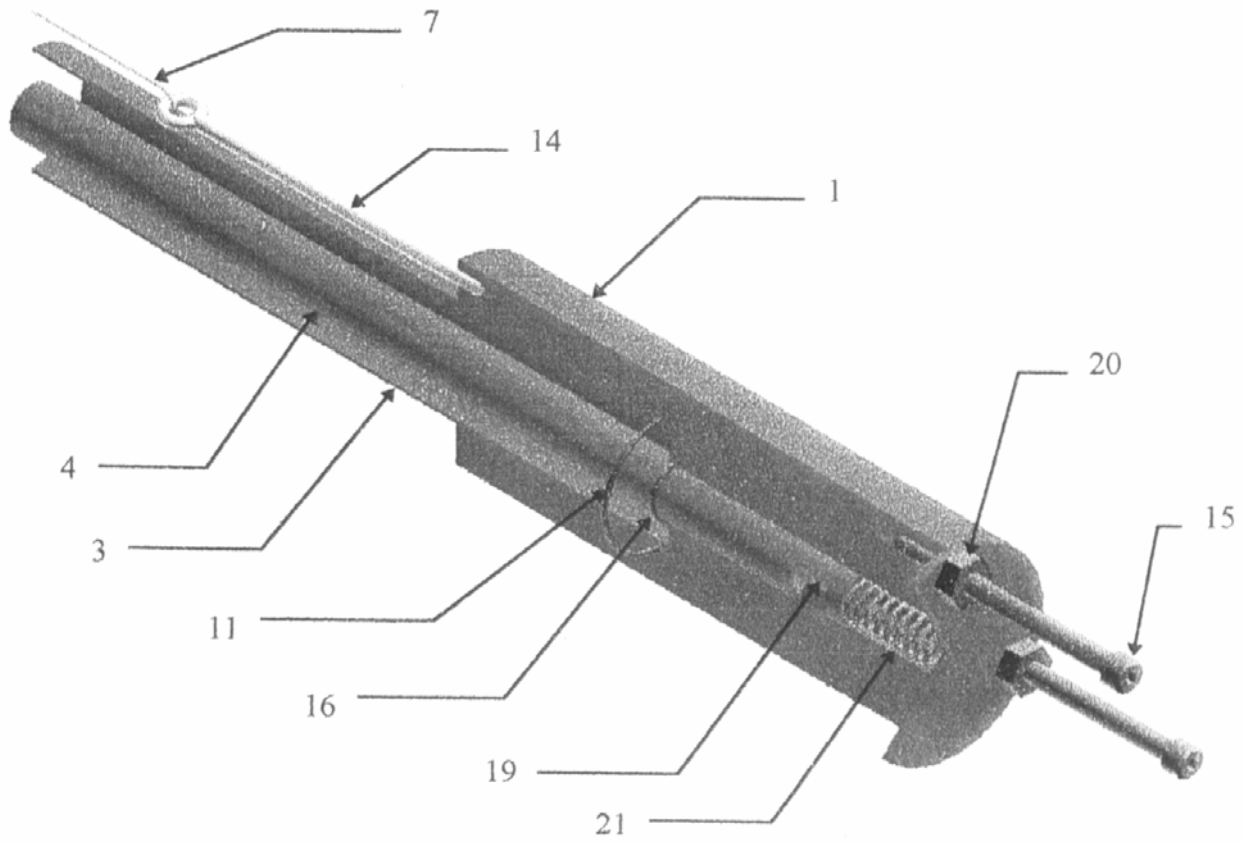


Figure 3.5. Planar short circuit.

The TDR mode version of the apparatus has a single expansion cone on the input side and a high quality planar short circuit termination at the far end. The planar short circuit is shown in detail by Figure 3.5. Conductive O-ring seals (items 11 and 16 on Figure 3.5) are used to provide low resistance and inductance electrical continuity to the planar surface and to prevent leakage of liquid samples out of the apparatus. A compression coil spring maintains constant force on the inner tube while the constant force on the outer tube is provided by three external coil springs. The use of coil springs on both inner and outer lines maintains constant electrical contact of all conductor surfaces during the measurement.

## **B. Instrumentation Setups and Raw Data**

We next describe the measurement procedures and electronic instrumentation setups in more detail. We start by describing the setup for transmission mode measurements using the impulse waveform. Referring to Figure 3.2, the measurement pulse is generated by the PSPL (Picosecond Pulse Labs) model 4015C pulse generator. The pulse generator is triggered at a constant 100 kHz pulse repetition frequency by a synchronizing system clock pulse from the Tek (Tektronix) 11801 sampling scope display unit. The 4015C output pulse drives the PSPL 4015RPH remote pulse shaping head to produce a 4.0 volt step pulse with a 20 picosecond transition time. The step pulse is converted to an approximate impulse by a hardware differentiator. The impulse has a width of  $< 30$  picoseconds FWHM and an output level of approximately 1 volt. The impulse passes through a 3 dB attenuator and a 15.2 cm (6 in) Goretex port cable to the input of the coaxial transmission line test fixture. The use of short high quality cables is essential in order to maintain measurement accuracy. The measured response for the complete apparatus is 46 picoseconds FWHM for air-filled line. The 46 ps response includes the combined effects of pulse source, differentiator, coaxial transmission line test fixture, cables, attenuators, and sampling head.

An input transition section allows the wave to expand from the input connector diameter before entering the dielectric sample. The plane wave passes through the sample and out of the opposite side. Reflections occur at each air dielectric interface. For an air-water interface, where water has a refractive index of 9, the reflection coefficient is 0.8. The reflected wave propagates back toward the source where it can then reflect again back into the measurement zone. The attenuators at the input and output help to absorb these reflected waves. Multiple reflections within the dielectric sample occur, but these are generally outside the time window of observation, and, therefore, do not effect our measurements. The multiple reflections, however, do contain additional information about the dielectric properties which can be analyzed.

After passing through the sample, the primary pulse propagates through the air line and output matching section. The pulse then passes through a 22.9 cm (9 in) semi-flex cable, 3 dB attenuator, and into the feedthrough sampling head where it is digitized.

The Tektronix type SD20 feedthrough sampling head, which has a 17 picosecond risetime, is terminated by a 3.5 mm, 50 ohm termination. The sampling head is operated in a vertical compartment of a Tektronix 11801 sampling scope display unit. We average 4,096 waveforms for each data record and sample 5,120 data points per waveform. This high degree of

over-sampling gives the quality data required for accurate numerical processing. When a complete waveform record has been averaged, the data is recorded to disk on a 486DX2 personal computer using Docuwave software.

The transmission mode measurement can also be made using a step function waveform by removing the hardware differentiator so that the step pulse from the 4015RPH is injected directly. In this case the input and output attenuators each have a value of 10 dB, rather than 3 dB, in order to limit the signal level applied to the sampling head to a safe level and to provide additional attenuation of reflections. Otherwise, operation with the step waveform is identical to impulse mode.

A typical measurement consists of collecting waveform records for a number of different dielectric sample lengths ( $L_{\text{sample}}$ ). By comparing the transmitted waveform for two different sample lengths, we can determine the propagation properties for a length of dielectric equal to the difference between the two sample lengths. Because this is a differential measurement, instrumentation system response and Fresnel losses are canceled. The total active length of the coaxial propagation test fixture is 100.0 cm, and the air path length is 100.0 cm less the sample length ( $L_{\text{sample}}$ ). The data must be corrected for the changes in air path length as sample length is changed.

The differential measurement is sensitive to the sample length. We calculate this length precisely to an accuracy of 0.1 cm by filling the line with the dielectric material using a 100 ml graduated cylinder and calculating  $L_{\text{sample}}$  (the length of the dielectric sample) from its measured volume. The known samples used in the demonstration were high purity (once-distilled) water.

Typical raw oscilloscope data resulting from transmission mode measurements with impulse excitation are shown in Figure 3.6. Four different waveforms resulting from propagation through four different lengths of water (2.39, 4.77, 19.10, and 76.39 cm) are shown. The traces are all at a time scale of 500 picoseconds/division, but the oscilloscope trigger delay time has been shifted to cause all the pulses to roughly overlap. The shortest length of propagation through the dielectric gives the narrowest impulse. The pulse width increases with increasing propagation length. The time shifts required to overlap the waveforms correspond closely with the time shifts calculated from the known dielectric constant of 81 for water. We note that it is necessary to account for the change in air path length as well as the change in water path length to properly account for time delays. There are secondary reflections visible in the data of Figure 3.6 for the three shortest length cases. These multiple reflections occur exactly at the expected times. The time window used for the analysis given in the following sections does not include the secondary reflections.

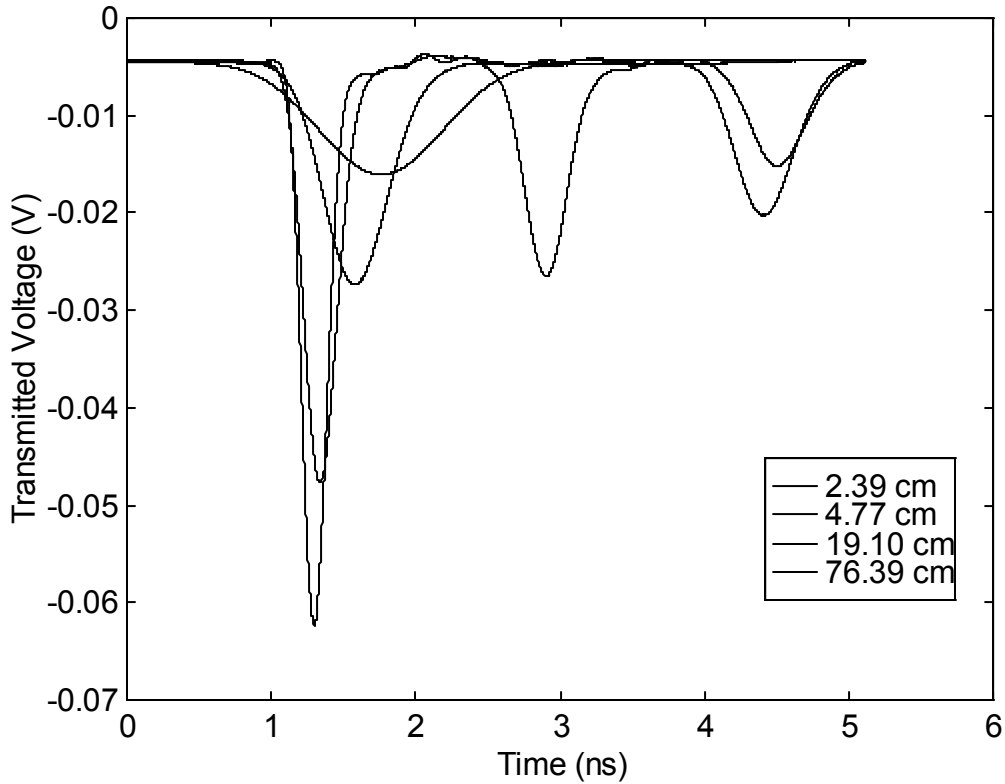


Figure 3.6. Raw data for the impulse transmission measurement, for water columns of varying lengths.

Table 3.1 summarizes data from eight different impulse transmission measurements, including the four which were plotted in Figure 3.6. The pulse width is seen to increase smoothly with propagation length from 46 ps for 0.0 length (air-filled line) up to 1018 ps for 76.39 cm length of water. At the same time, the amplitude decreases with propagation length. This is exactly the behavior we expect from a classical Debye material where the pulse width increases and the amplitude decreases continuously with propagation range through the medium. In a following theoretical section it will be shown that the measured waveforms are very well described by the classical Debye model for water using published values for  $\epsilon_s$ ,  $\epsilon_\infty$  and  $t_o$ , which are the three Debye parameters. This close agreement with theory and published data for distilled water gives us confidence that the apparatus is working well and will give good data on the unknown samples which are to be studied later.

Data was also taken in transmission mode using a step function waveshape. The water level for these experiments was measured with a dip stick, which is not as accurate as the method using a graduated cylinder. We estimate the length of the dielectric sample was measured to within 0.7 cm for this experiment.

TABLE 3.1. EXPERIMENTAL DATA FOR IMPULSE TRANSMISSION THROUGH DISTILLED WATER

Water Length (cm)	Scope Delay (ns)	Pulsewidth (FWHM ps)	Amplitude (mV)
0.00	82.17	46	494
1.19	82.37	158	76.2
2.39	82.67	204	58.0
4.77	83.27	271	43.2
9.55	84.47	376	31.5
19.10	86.82	522	22.8
38.19	91.62	722	16.2
76.39	101.72	1018	11.7

$$\text{Air Length} = 100.00 \text{ cm} - \text{Water Length}$$

Typical raw oscilloscope data resulting from the transmission mode measurement with step function excitation is shown in Figure 3.7. Four different waveforms resulting from propagation through an air path and three different lengths of water (32.4 cm, 70.5 cm, and 93.3 cm) are shown. The traces are all at a time scale of 500 picosecond/division, but the oscilloscope trigger delay time has been shifted to cause the leading edge of the pulses to overlap. The transmitted amplitude is higher for the air path waveform, since Fresnel losses do not occur for air alone. The data displays the expected behavior for classical Debye material. The pulse risetime is seen to increase with propagation length, while the final amplitude reached does not depend on the length of propagation. The transmitted step function waveform eventually reaches full amplitude. The measured transmission coefficient agrees with the theoretically calculated value of 0.36 for a wave passing through a dielectric slab with relative dielectric constant of 81. The time shifts required to overlap the leading edge of the waveforms also correspond closely with the time shift calculated for a dielectric constant of 81 for water. Table 3.2 summarizes data for four different measurements which were shown in Figure 3.7.

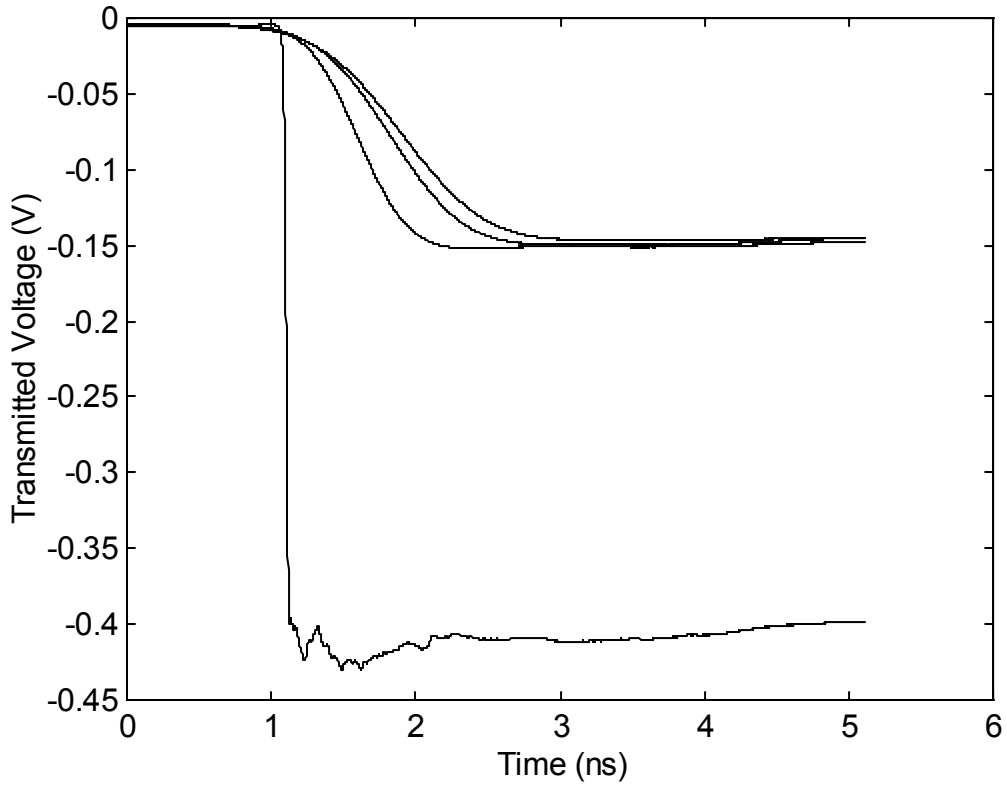


Figure 3.7. Raw data for the step transmission measurement

TABLE 3.2. EXPERIMENTAL DATA FOR STEP PULSE TRANSMISSION THROUGH DISTILLED WATER

Water Length (cm)	Scope Delay (ns)	Risetime (10% - 90% ps)
0.00	82.04	48
32.4	90.04	690
70.5	99.24	1006
93.3	105.59	1155

Air Length = 100.00 cm – Water Length

## IV. Results

We consider here the results of the processing to extract the complex dielectric constant,  $\epsilon_r$ , from the transmission data described in the previous section. In particular, we describe the processing for two columns of distilled water, with lengths of 2.39 cm and 9.55 cm,. The transmission method was used, with an impulse waveshape.

A plot of the measured impulse waveform is shown in Figure 4.1. This is simply the signal transmitted through the coaxial test fixture, with no sample. The transmitted impulse has the frequency domain spectrum shown in Figure 4.2. Note that this signal is not used in any of the analysis. We present it here to demonstrate the bandwidth of the instrumentation.

Plots of the transmitted signals for 2.39 cm and 9.55 cm of water are shown in Figures 4.3 and 4.4. To process these two waveforms, we convert them to the frequency domain and take the ratio of the waveform through the longer water column to that through the shorter water column. When taking this ratio, we limit the magnitude of the denominator to be no smaller than 0.01 times its maximum magnitude, in order to avoid dividing by very small numbers. After taking the ratio, we apply a 10<sup>th</sup>-order modified Butterworth filter, as described in [4], with a cutoff frequency of 4 GHz. The resulting frequency domain ratio is shown in Figure 4.5. This is the relative frequency domain impulse response for propagation through 7.16 cm of distilled water, when compared to propagation through the same length of air. The time domain impulse response is shown in Figure 4.6, and its integral is plotted in Figure 4.7. Also plotted in Figures 4.5 through 4.7 are the expected curves, using the Debye model (eqn. 2.7). Quite good agreement is seen when these measurements are compared to the theory. Note that our measurements are all absolute (not relative), and there has been no adjustment for either time delay or amplitude to match to the theory.

Next, we convert the measurements to a dielectric constant, using the algorithm described in Section II. The real and imaginary parts of the dielectric constant are shown in Figure 4.8, along with the curves expected from the Debye model. Our measurements follow the theory quite well, and they follow the bend in the curves that is expected above 1 GHz. Finally, we convert the complex dielectric constant to attenuation, in Figure 4.9. Again, the agreement with theory is quite reasonable.

With the results we have seen so far, we get results only as low as 667 MHz. The reason for this is that we have had to use relatively short columns of water, in order to measure a enough high frequencies. To get more low frequency, we repeated the measurement with longer water columns, with lengths 9.55 cm and 76.39 cm. The raw data is shown in Figures 4.10 and 4.11. With the longer time window, we can now provide measurements as low as 200 MHz.

To process the second set of data, everything is implemented the same as before, with the exception that the cutoff frequency of the filter is 1 GHz. The results for dielectric constant are shown in Figure 4.12, and the corresponding attenuation is shown in Figure 4.13. Once again, our agreement with theory is quite good.

Taken together, Figures 4.8 and 4.12 demonstrate that we can measure  $\epsilon_r$  to a few percent over a broad frequency range. The data of Figures 4.9 and 4.13 demonstrate accurate measurement of attenuation coefficients between 0.05 dB/cm and 10 dB/cm. Note that distilled water has a higher attenuation than many of the samples we will test later, so it provides a fairly severe test of the apparatus. Other dielectric samples with less dispersion and lower attenuation will be measured over a broader frequency range.

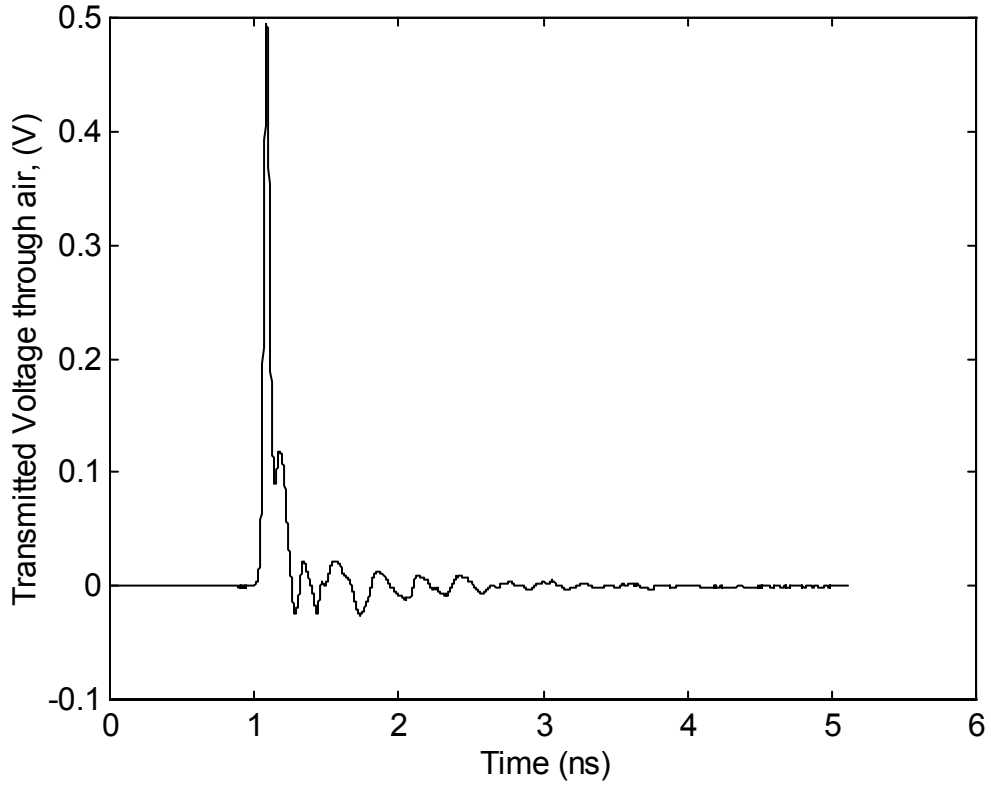


Figure 4.1. Transmitted waveform with no sample, 100 cm of air.

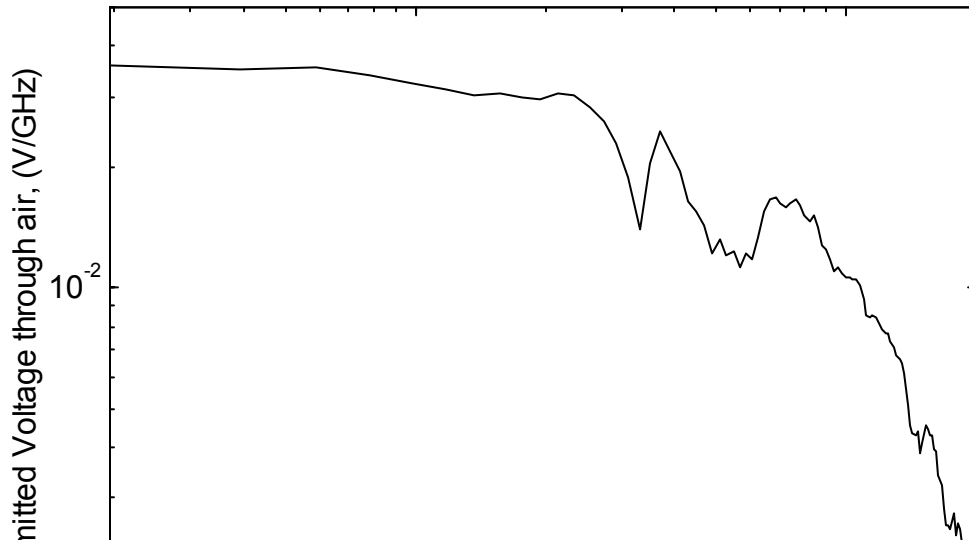


Figure 4.2. Frequency spectrum of the signal in Figure 4.1.

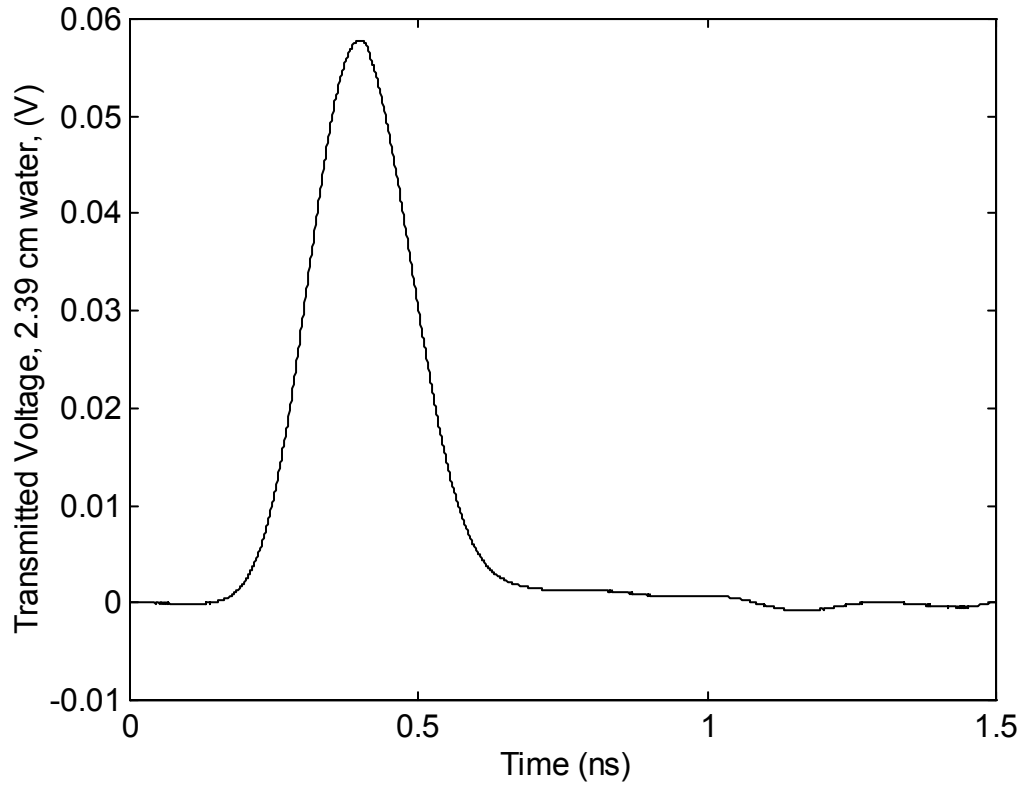


Figure 4.3. Signal transmitted through 2.39 cm of distilled water

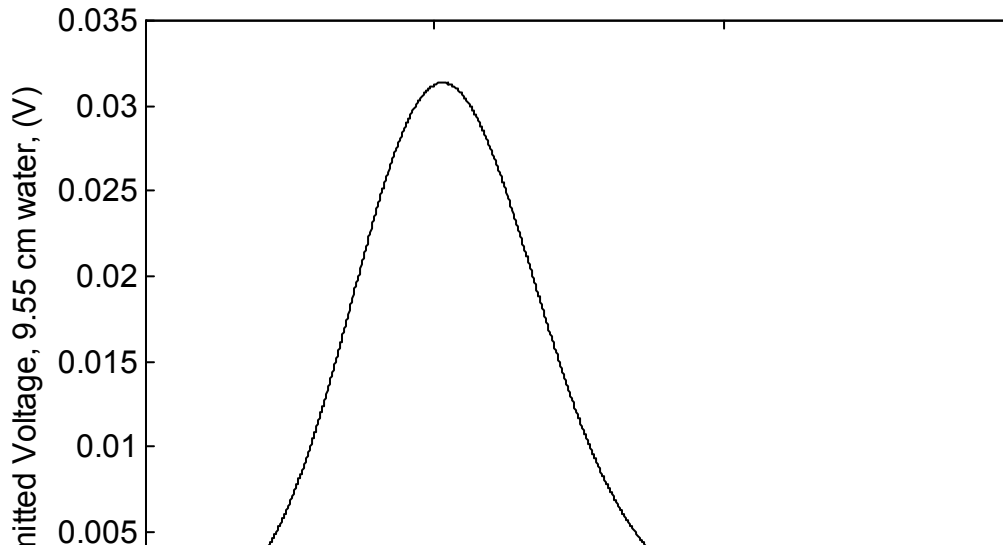


Figure 4.4. Signal transmitted through 9.55 cm of distilled water

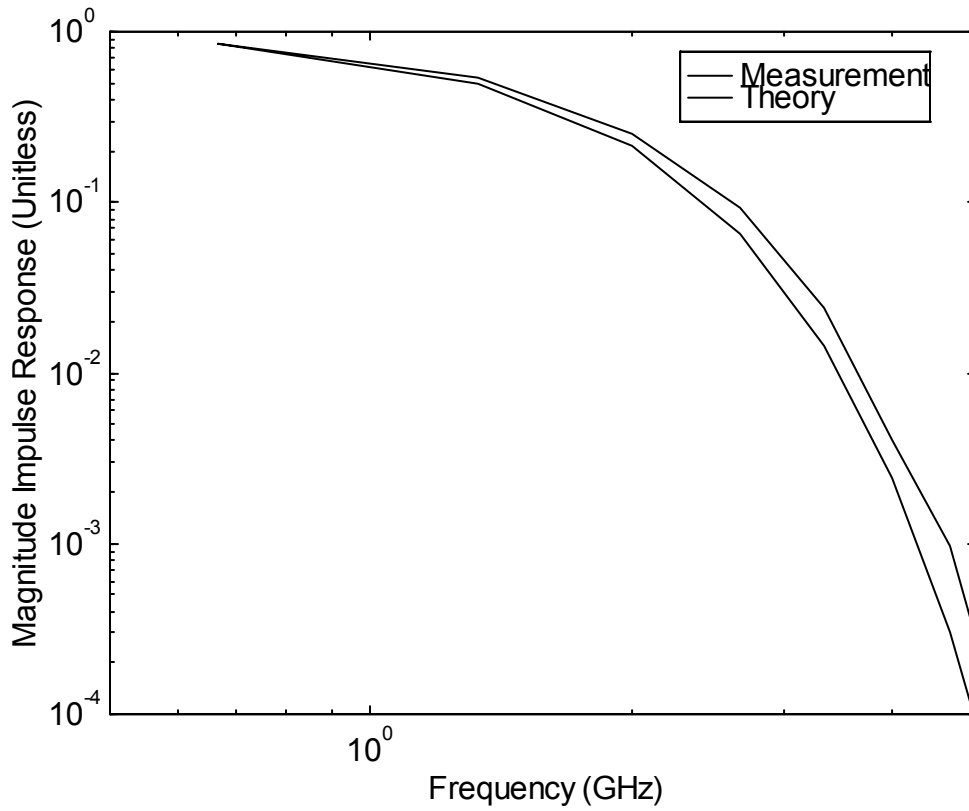


Figure 4.5 . Impulse response spectrum for propagation through 7.16 cm of water.

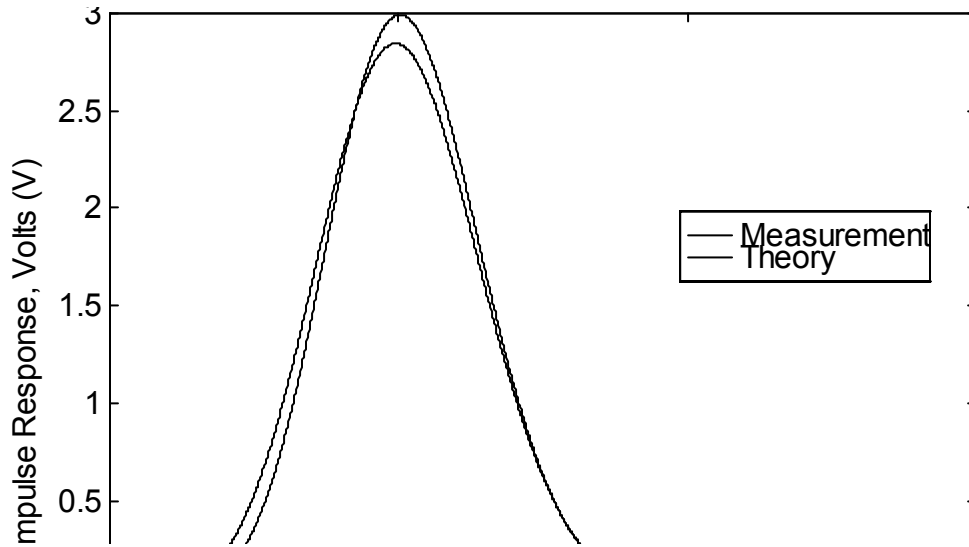


Figure 4.6. Impulse response for propagation through 7.16 cm of water.

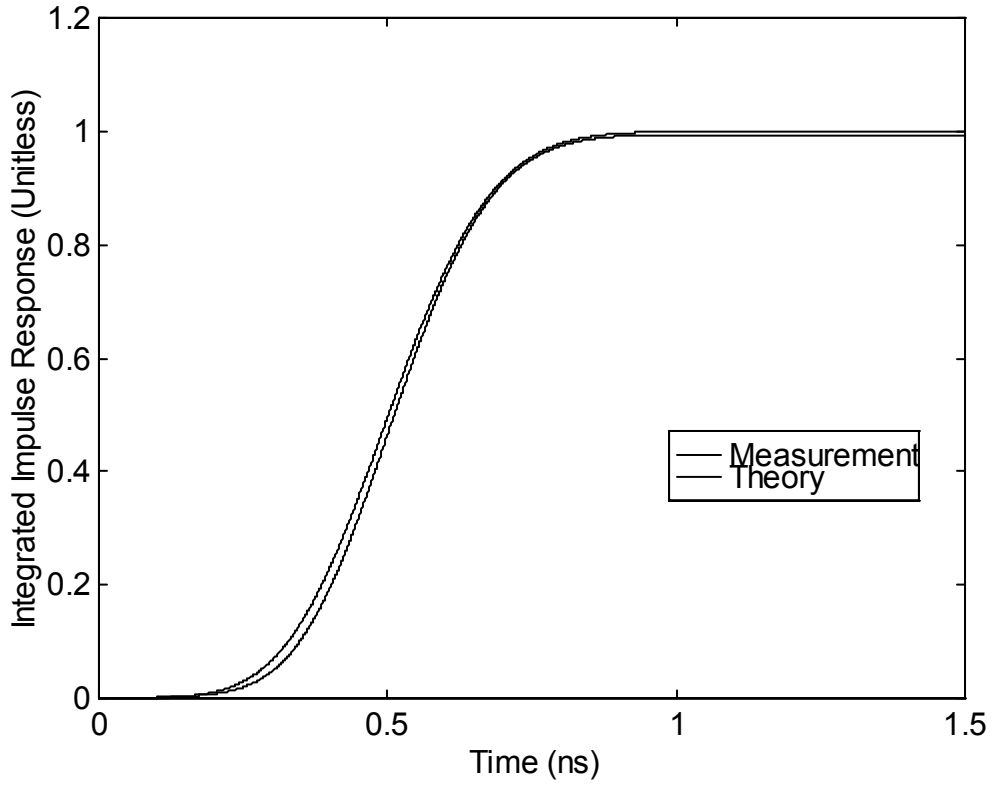
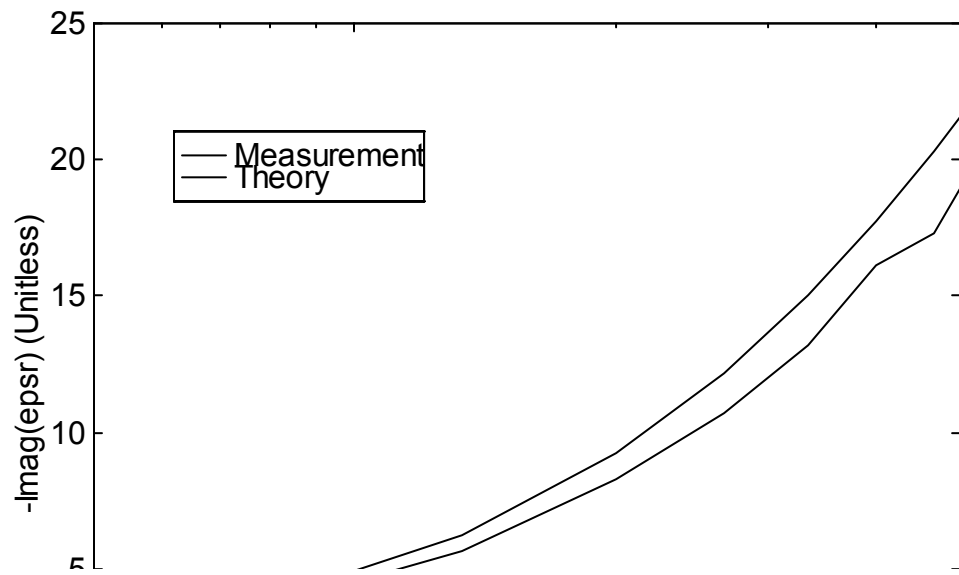
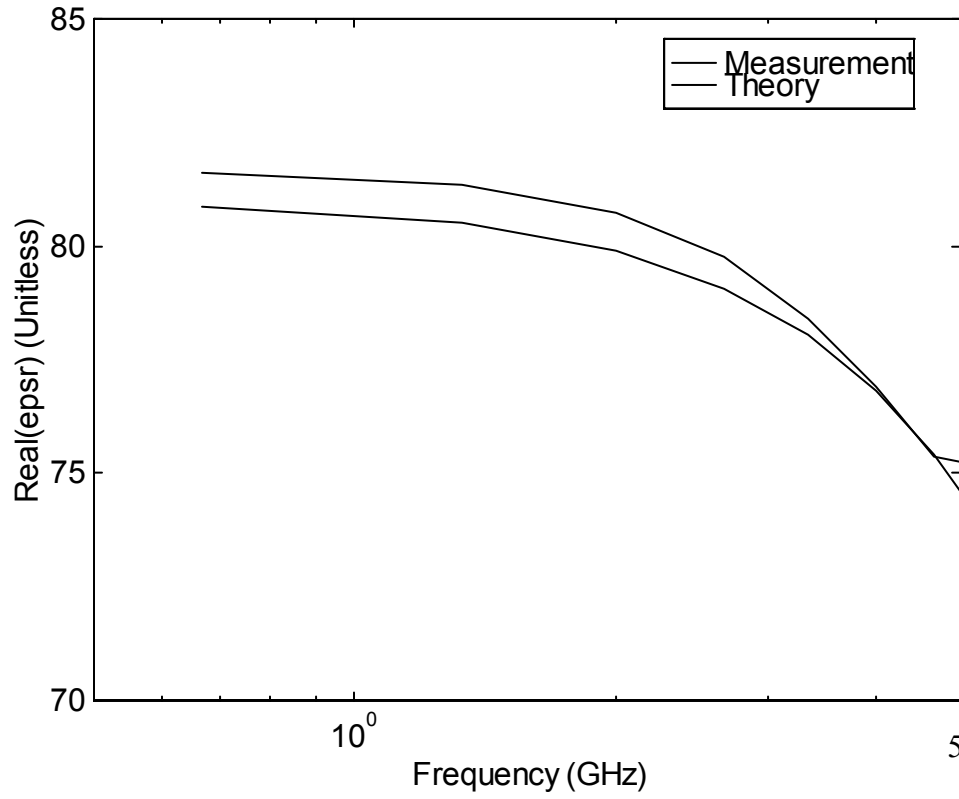


Figure 4.7. Integral of the impulse response for propagation through 7.16 of water.



5

Figure 4.8. Real (top) and imaginary (bottom) parts of the measured dielectric constants of distilled water, measured with water columns 2.39 and 9.55 cm in length..

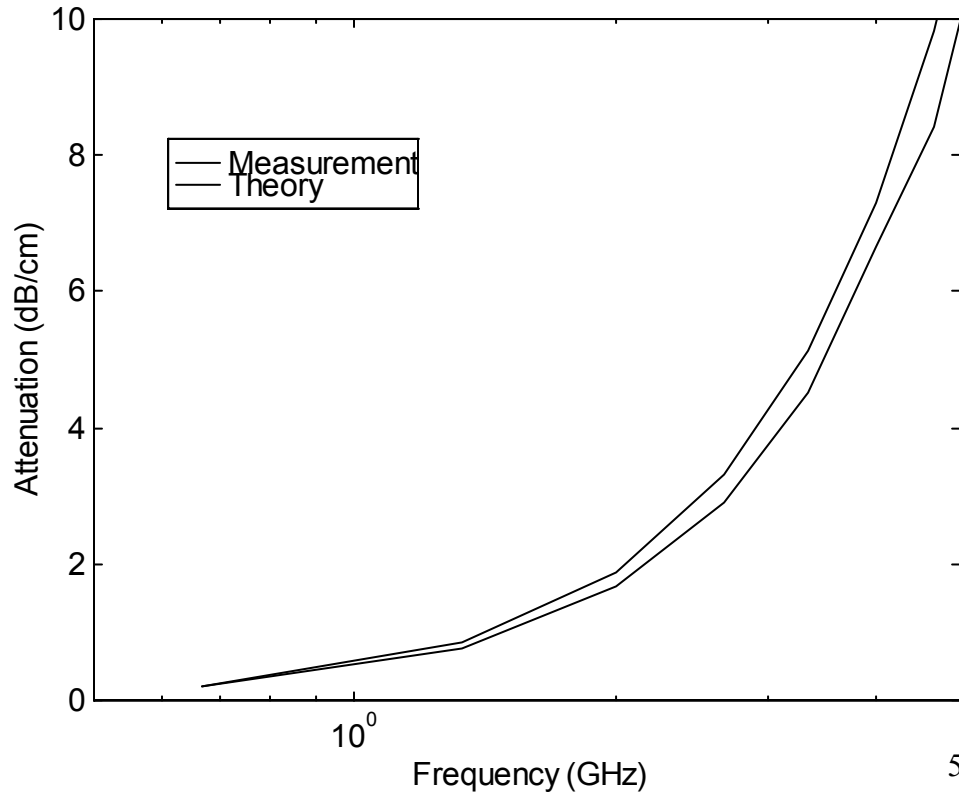


Figure 4.9. Attenuation coefficient of distilled water, measured with water columns 2.39 and 9.55 cm in length.

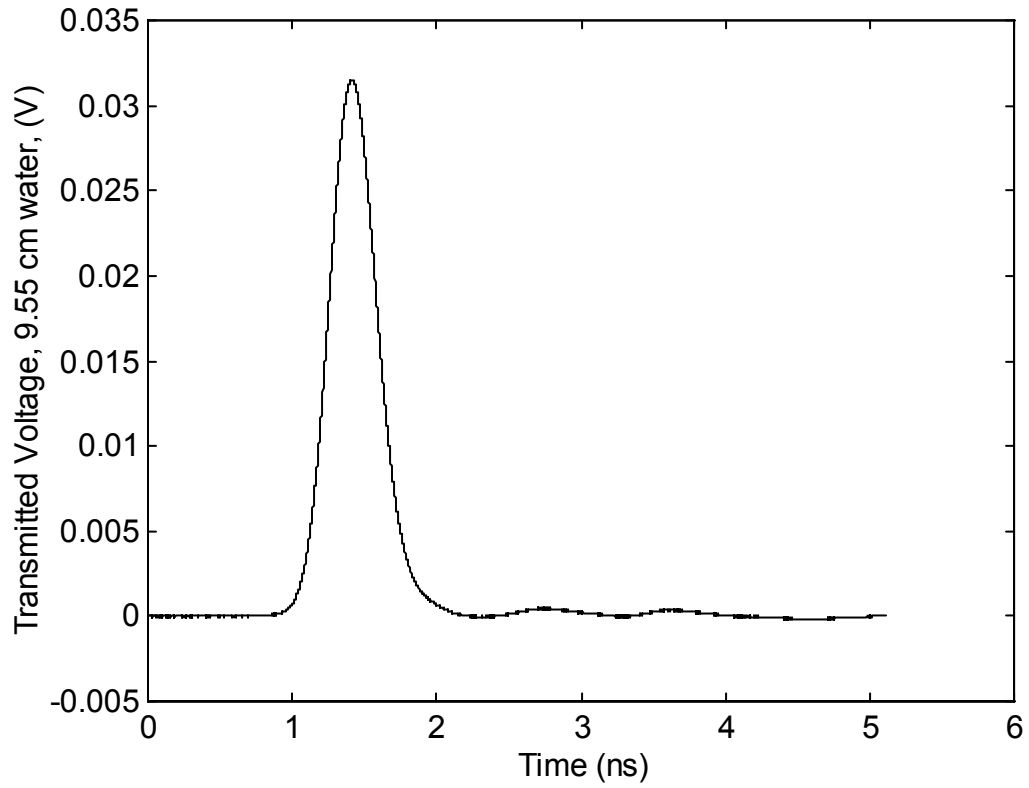


Figure 4.10. Signal transmitted through 9.55 cm of distilled water

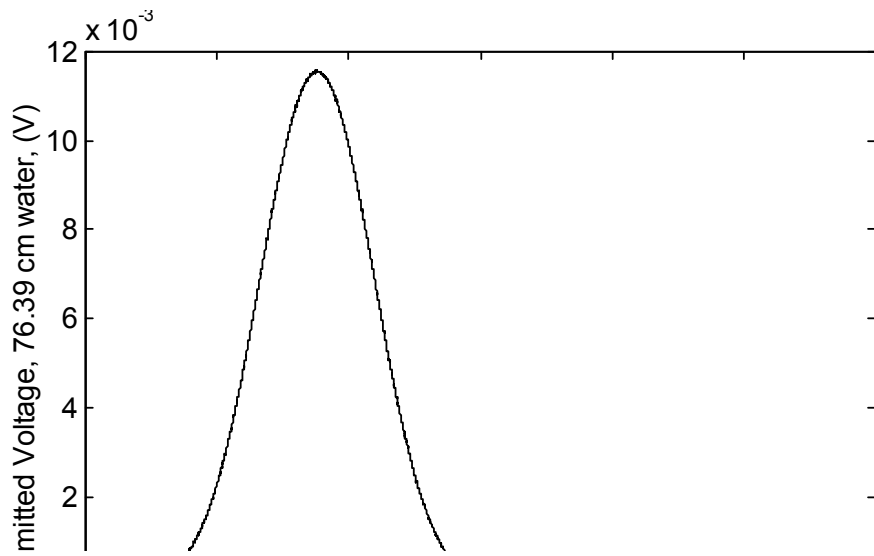


Figure 4.11. Signal transmitted through 76.39 cm of distilled water

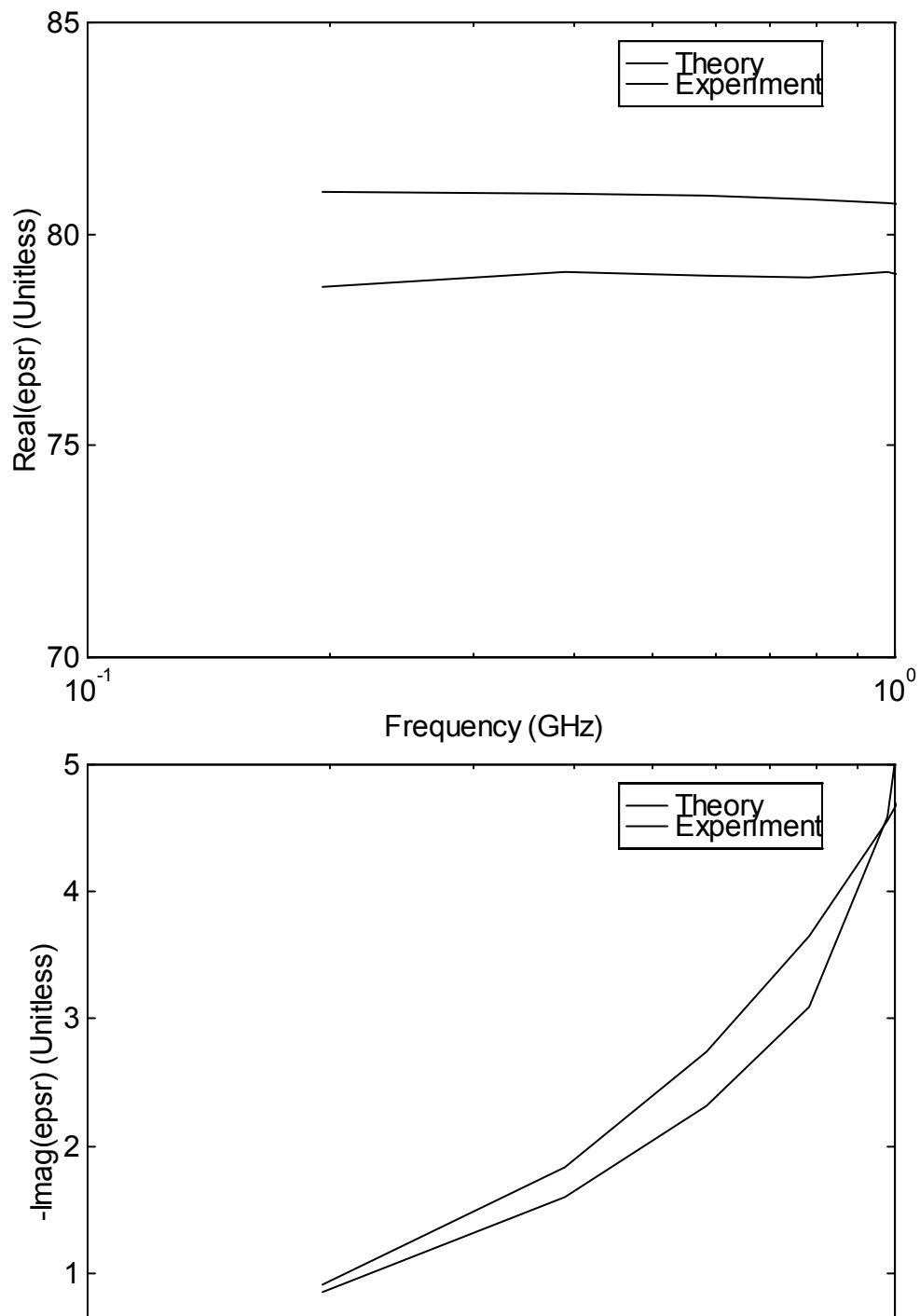


Figure 4.12. Real (top) and imaginary (bottom) parts of the measured dielectric constants of distilled water, using water columns 9.55 and 76.39 cm in length..

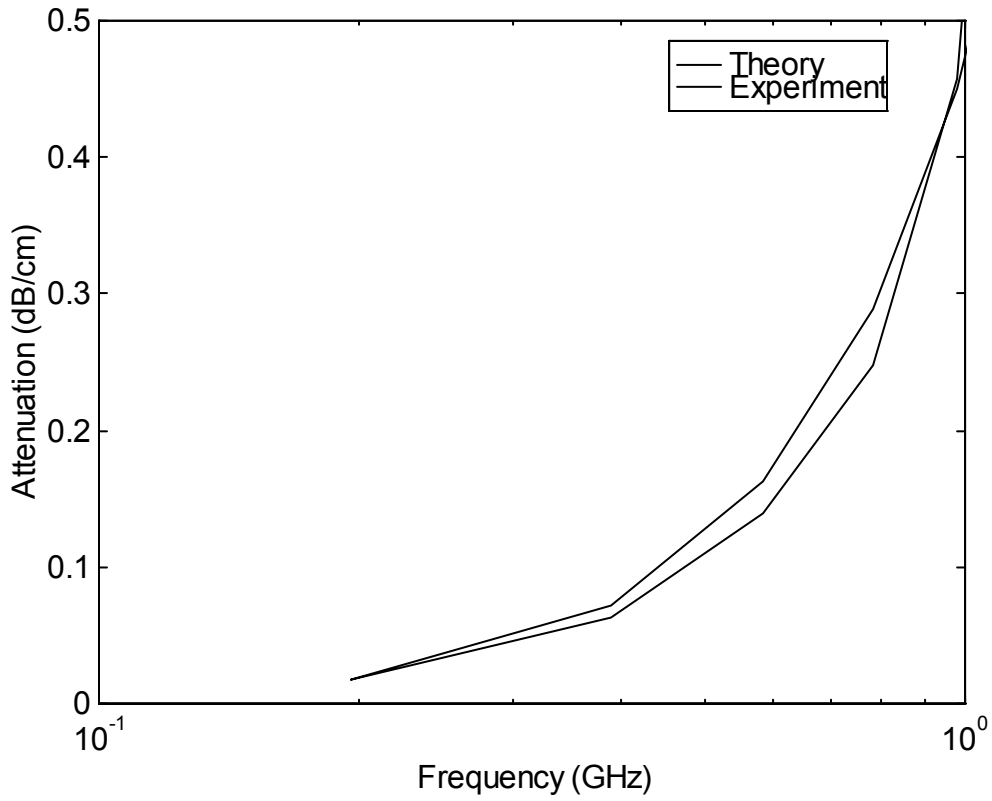


Figure 4.13. Attenuation coefficient of distilled water, measured with water columns 9.55 cm and 76.39 cm in length.

## V. Conclusion

We have built and demonstrated a coaxial test fixture capable of measuring complex dielectric constants for materials with high loss. The test fixture has been demonstrated with distilled water, and good agreement was achieved with theory. In a later note we will provide measurements of other materials.

## Acknowledgment

We wish to thank Dr. Kwang Min, of Wright Laboratory / MNMF, for funding this work.

## References

1. A. M. Nicolson and G. F. Ross, "Measurement of the Intrinsic Properties of Materials by Time-Domain Techniques," *IEEE Trans. Instrumentation and Measurement*, Vol. IM-19, No. 4, November 1970, pp. 377-382.
2. C. Courtney, W. Motil, T. Bowen, and S. Blocher, Measurement Methods and the Characterization of the Electromagnetic Properties of Materials, Measurement Note 48, December 1996
3. K. S. Kunz, and R. J. Luebbers, *The Finite Difference Time Domain Method for Electromagnetics*, CRC Press, Boca Raton, 1993, pp. 124-128.
4. E. G. Farr and C. A. Frost, Compact Ultra Short Pulse Fuzing Antenna Design and Measurements, Sensor and Simulation Note 380, June 1995.